Electrochimica Acta 381 (2021) 138242

Contents lists available at ScienceDirect

Electrochimica Acta

journal homepage: www.elsevier.com/locate/electacta

Electrochemical oxidation of 4-ethynylaniline: A green electrochemical protocol for the synthesis of diazine compounds

Maryam Mehrdadian[a], Sadegh Khazalpour[a,*], Ameneh Amani[b], Mahdi Jamshidi[a]

[a] Department of Analytical Chemistry, Faculty of Chemistry, Bu-Ali Sina University, Hamedan 6517838683, Iran
[b] Department of Chemistry, University of Nahavand, Nahavand, Iran

ARTICLE INFO

Article history:
Received 3 December 2020
Revised 1 February 2021
Accepted 21 March 2021
Available online 31 March 2021

Keywords:
Electrochemical oxidation
4-ethynylaniline
Cyclic voltammetry
Diazines
Electrosynthesis

ABSTRACT

Electrochemical oxidation of 4-ethynylaniline was studied in buffer solution/acetonitrile mixture in different pHs. Our electrochemical data assert that the product of oxidation of 4-ethynylaniline is unstable in acidic and alkaline solution, and can be hydrolyzed in strong acidic (pH: 1–3) and alkaline (pH: 9–10) solutions. In continues, the electrochemical synthesis of 1,2-bis(4-ethynylphenyl)diazene was carried out by electrochemical oxidation of 4-ethynylaniline in aqueous HCl buffer and in a simple undivided cell, using carbon anode. To biological assessment (antibiotic activity), the molecular docking of some receptors and 1,2-bis(4-ethynylphenyl) diazene have been performed. The negative values of the binding affinity showed that azo product has an inhibitory effect against receptors. Also, the diffusion coefficient of 4-ethynylaniline in acetonitrile was determined using the single potential-step chronoamperometry technique.

1. Introduction

Heteroaryl acetylenes are important structures in the synthesis of organic compounds as well as in materials science [1]. These compounds are considered to be adaptive structures due to their multiple structures based on a carbon-carbon triple bond. Recently, much attention has been focused on chemical transformations to the direct oxidation of carbon-carbon double and triple bonds using electrolysis [2,3].

Ethinyl anilines, as a group of heteroaryl acetylenes, are widely used in materials science, especially as a strong electron donor for applications in optoelectronic devices and their ability to the formation of a diazonium compound and doing the polymerization reaction [4–6]. Also these compounds as primary amines play a pivotal role in the synthesis of various substrates [7–9]. On the other hand, diazines (diazo compounds), with the general structure of R-N = N-R, are important families of compounds in chemistry. In this category of compounds, the azo-aromatic type is more stable, which is due to the fact that the N = N group is part of a large delocalized system consisting of arene groups [10]. Azo aromatic compounds are widely used in various fields [11–13]. These compounds play an important role not only in analytical chemistry [14], but also in dye industry applications, acid-base detectors, initiators of radical reactions [15,16], food additives [17] stains in the histological and biological industries [18], and also take a role as inhibitors of tumor growth [19,20] and drug delivery agents [21–24]. Therefore, due to the importance of the N = N bond, especially in biologically active molecules and the need to develop new antibiotics, attention has been paid to the synthesis of new azo products [25]. 4-ethynylaniline, also known as *p*-alkynylaniline, has amino and ethynyl substitutions in the para position in the benzene ring. This compound is one of the important heteroaryl acetylenes (Fig 1).

Due to the properties of 4-ethynylaniline compound and especially its ability to formation a diazonium compound and in continuation of our interest in the electrochemistry of organic compounds [26–28], in this work at the first step, we investigated the electrochemical oxidation of 4-ethynylaniline (**4-EA**) completely by cyclic voltammetry, differential pulse voltammetry and controlled potential coulometry techniques at the various pHs. In the following, the electrochemical synthesis of 1-(4-aminophenyl)ethan-1-one **(P1)** and 1,2-bis(4-ethynylphenyl) diazene (**P2**) were successfully carried out in an aqueous HCl buffer. To biological assessment, the molecular docking study of some receptors that have powerful interactions with 4-aminoacetophenone has been performed. The diffusion coefficient of 4-ethynylaniline in pure acetonitrile was determined using the single potential-step chronoamperometry technique.

* Corresponding author.
E-mail address: S.Khazalpour@basu.ac.ir (S. Khazalpour).

https://doi.org/10.1016/j.electacta.2021.138242
0013-4686/

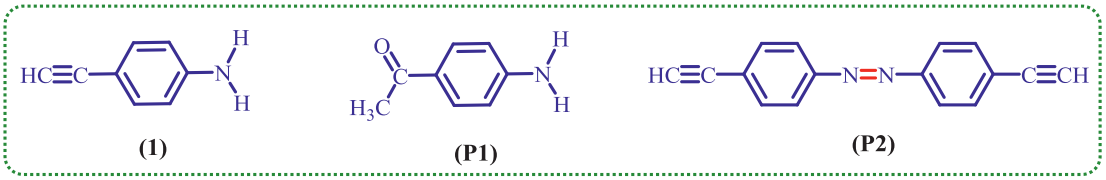

Fig 1. Structure of 4-ethynylaniline (**4-EA**) and synthesized compounds (**P1** and **P2**) in this study.

2. Experimental

2.1. Apparatus and reagents

Cyclic voltammetry and chronoamperometry were performed using an Autolab model PGSTAT 204 potentiostat/galvanostat, and controlled potential coulometry was performed using a Behpazhoh model 2051 potentiostat/galvanostat, respectively. The glassy carbon disc (1.8 mm diameter), platinum wire, and Ag/AgCl electrode were used as the working electrode, counter electrode, and the reference electrode in the voltammetry, respectively (all electrodes from AZAR Electrode Co.). Four carbon rods (6 mm diameter and 4 cm length) were used as the working electrode, and a stainless-steel grid was used as a counter electrode in controlled-potential coulometry.

2.2. Electroorganic synthesis of ***P2***

For electrolysis, 0.125 mmol of 4-ethynylaniline (**4-EA**) was added to an aqueous in HCl (0.1 M) in water /ethanol (70/30 v/v) solution and the electrolysis performed at 0.87 V versus Ag/AgCl in an undivided cell. The electrolysis was expired when the decline of the current became more than 95%. At the end of electrolysis, the solution's pH was 1.5 that reached 5.0 by saturated sodium bicarbonate solution, and then the products extracted using ethyl acetate. After extraction, the material was dried and then concentrated. Obtained precipitate was purified by thin layer chromatography on silica gel 60 HF254 (*n*-hexane/ethyl acetate, 1/2 *v*/*v*). The yellow fraction was corresponding to 1,2-bis(4-ethynylphenyl) diazene (**P2**). The separated product was characterized by M.p., IR, UV, ^{1}H NMR, ^{13}C NMR and MS.

1-(4-aminophenyl) ethan-1-one (P1) (C_8H_9N)

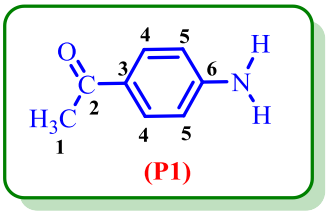

Creamy solid, Isolated yield: 26%. M.p.: 94–96 °C.^{1}H NMR (400 MHz, DMSO–d_6) δ (ppm): 2.38 (s, 3H, methyl), 6.01 (s, 2H, NH_2), 6.55 (d, J = 8 Hz, 2H, aromatic), 7.65 (d, J = 8 Hz, 2H, aromatic), ^{13}C NMR (100 MHz, DMSO–d_6) δ (ppm): 25.7 (C-1), 112.4 (C-5), 124.7 (C-3), 130.8 (C-4), 154.6 (C-6), 194.8 (C-2). IR (KBr) ν (cm-1): 3395, 3333, 1652, 1564, 1427, 1289, 1091.

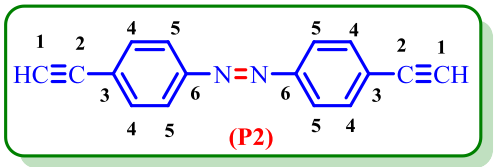

1,2-bis(4-ethynylphenyl) diazene (P2) ($C_{16}H_{10}N_2$)

Yellow solid, Isolated yield: 55%. M.p.: 184–188 °C (Dec.).^{1}H NMR (400 MHz, DMSO–d_6) δ (ppm): 3.81 (s, 2H, methylene), 6.58 (d, J = 8 Hz, 4H, aromatic), 7.16 (d, J = 8 Hz, 4H, aromatic. ^{13}C NMR (100 MHz, DMSO–d_6) δ (ppm): 76.9 (C-1), 84.9 (C-2), 107.4 (C-3), 113.3 (C-5), 132.2 (C-4), 149.4 (C-6). IR (KBr) ν (cm-1): 3486, 3388, 2097, 1595, 1440, 1305, 1283, 1215. MS (EI, 70 eV) *m/z* (relative intensity): 230 (M^+., 8), 43 (100), 57(92), 69 (82), 83 (68), 120 (50), 80 (62), 97 (62), 136 (27), 152 (18).

2.3. Molecular docking analysis

To biological assessment, the molecular docking study of the synthesized azo compound and some receptors that is expected to has a potentially high antibacterial property. The crystal structure of antibacterial target proteins, E. coli Topoisomerase IV (PDB ID: 3FV5), S. aureus Dihydrofolate Reductase (PDB ID: 3SRW), Gyrase B (PDB ID: 4ZVI), and beta-ketoacyl-acyl (PDB ID: 1HNJ) were chosen for the docking studies. Furthermore, BH32 alkylated (PDB ID: 6Q7N), OE1.3 alkylated (PDB ID: 6Q7R), OE1.2 (PDB ID: 6Q7P), and *R*-specific alcohol dehydrogenase (wild type) from Lacto Bacillus Brevis (PDB ID: 1ZK4) have been chosen for calculation of binding affinity between 4-aminoacetophenone and receptors via Molegro Virtual Docker (MVD) [29]. After extraction of the X-ray structure of receptors from a favorable biological database (PDB: https://www.rcsb.org), the structure of 4-aminoacetophenone and 1,2-bis(4-ethynylphenyl)hydrazine were draw and optimized using ChemBio Ultra software (version: 16.0, Cambridge Soft). Before docking, some preparing works such as adding polar hydrogens to enzyme structures, removing water molecules, cofactors, and ligands should be performed. The parameter settings in the software package were as following: Score function: MolDock Score as the score function; Ligand evaluation: Internal ES, Internal HBond, Sp2–Sp2 Torsions, all checked; Number of runs: 30 runs; Algorithm: MolDock SE; Max. steps: 300; Max. population size: 50; Neighbor distance factor: 1.00; Maximum Interactions: 1500; Max. the number of poses returned: 20).

3. Results and discussion

3.1. Electrochemical oxidation of 4-ethynylaniline (4-EA): the effect of pH

The cyclic voltammograms of the 4-ethynylaniline (**4-EA**) (1.0 mM) in buffered solutions with various pHs (c = 0.2 M) /acetonitrile (80/20 v/v) are illustrated in Fig. 2.

In Fig. 2, pHs 1.0, 2.0, and 3.0 cyclic voltammograms exhibit two dependent anodic peaks (A_1 and A_2). Anodic peak A_1 corresponds to the electrooxidation of **4-EA** to the corresponding oxidation form within an irreversible process. The product of these oxidation enters in the hydrolysis reaction. The second anodic peak, A_2, corresponds to the electrooxidation of the product of the hydrolysis reaction. With increasing pH as well as increasing the potential scan rate, A_2 decreases and disappears (Figs. 2, 5 and 1S). Anodic peak A_2 reappears in basic solutions (pH>8) (Fig. 2S).

As can be seen (Fig. 2), the electrochemical oxidation of **4-EA** is pH dependent process, and hence the peak potential for peak A_1

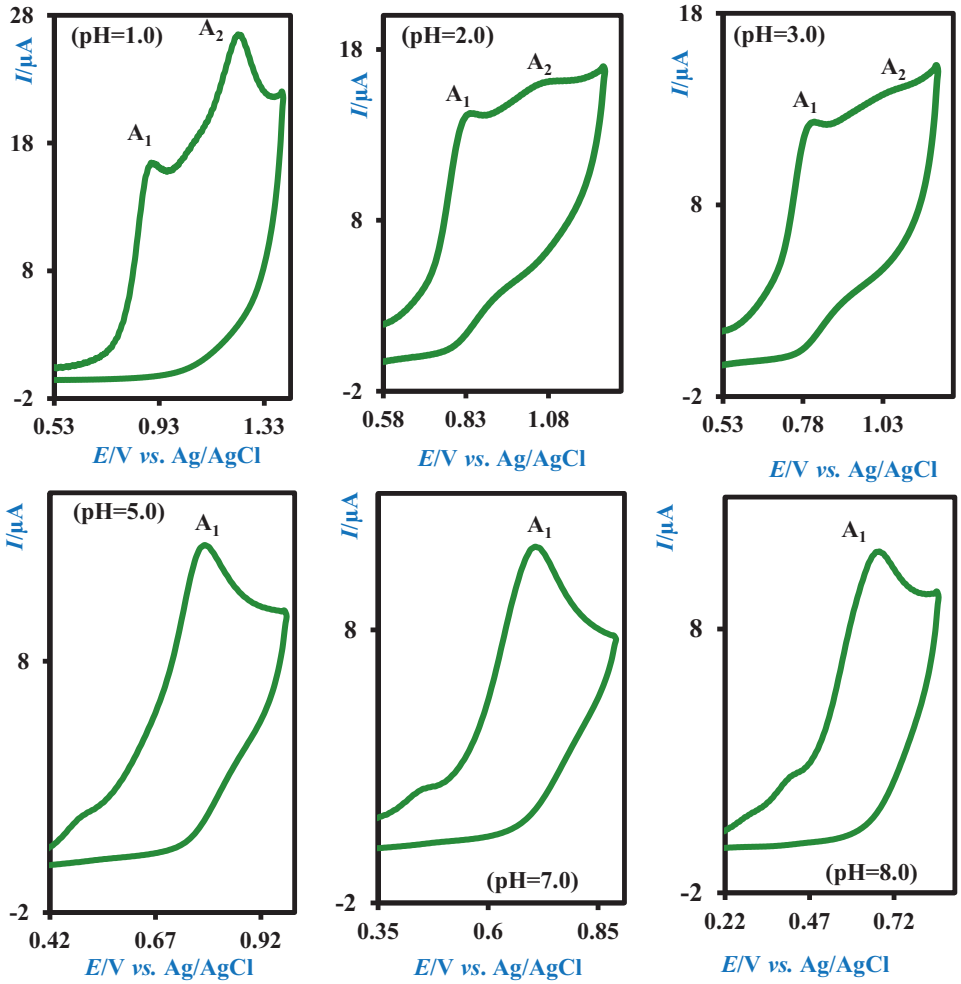

Fig. 2. Cyclic voltammograms of 4-ethynylaniline (**4-EA**) (1.0 mM) at the surface of glassy carbon electrode in buffered solutions with various pHs and same ionic strength (c = 0.2 M) /acetonitrile (80/20 v/v). Potential scan rate: 100 mV/s. Room temperature.

(E_p^{A1}) shifted to the less positive potentials by increasing pH. Since the proton(s) participate in the oxidation reaction of **4-EA**, this is a predictable phenomenon. Whereas in our experimental conditions, anodic peaks A_1 and A_2 are nearly close together, we decide to use the differential pulse voltammetry for the well assigning the peak potential (E_{pA1}) and drawing the E-pH diagram. A potential-pH diagram is created by drawing the E_{pA1} against pH values in Fig 3. Because of the taking of proton(s) apart in the oxidation of **4-EA**, E_{pA1} turned over to the less positive potentials by incrementing pH. The linear regression equation is:

$E'_{PA1} = E_{pA1(pH=0)}$-(2.303mRT/2F) pH where $E_{pA1(pH=0)}$ is the peak potential for peak A_1 at pH = 0.0, m is the number of protons take apart in the reaction. R, T, and F have their usual meaning. The E_{pA1}-pH diagram includes two linear sections with different equations and slopes around pH values 4.9.

In pH <4.9:

E'_{PA1} = 0.83- 0.02 pH or slope =20 mV/pH

In pH >4.9:

E'_{PA1} = 0.99–0.053 pH or slope =53 mV/pH

These results show that three different forms of **4-EA** can be produced in the diffusion layer with the variation of pH and electrode potential. One of these forms is a reduced form, and two others are oxidized forms.

According to the obtained linear slopes in the Fig. 3, it can be concluded that the electrode reaction at pH ⟨ 4.9 is a two-electron/one-proton and pH ⟩ 4.9 is a two-electron/two-proton process. At pH < 4.9, the protonated **4-EA** was oxidized to 2-(4-iminiocyclohexa-2,5–dien-1-ylidene)ethen-1-ylium (**4-EA$_{ox}$H$^+$**) and at pH>4.9 it oxidized to 2-(4-iminocyclohexa-2,5–dien-1-ylidene)ethen-1-ylium (**4-EAox**) (Scheme 1). In addition, the calculated *pK*a for the **4-EAoxH+**/**4-EAox** equilibrium is 4.9 (Scheme 2).

3.2. Electrochemical oxidation of 4-EA in strongly acidic and basic media. investigation of the hydrolysis reaction

Fig. 4, shows the differential pulse voltammogram of **4-EA** (1.0 mM) at 10 mV/s, in mixture of 0.1 M HCl /acetonitrile(80/20 v/v). As shown, the voltammograms have two dependent anodic peaks (A_1 and A_2) in a positive scan. These anodic peaks (A_1 and A_2) are appurtenant to oxidation of protonated form of **4-EA** (**4-EAH$^+$**) to **4-EA$_{ox}$H$^+$** (Scheme 1) and oxidation of the product obtained of the hydrolysis reaction, respectively, under the experimental conditions.

To further and exactly examination of the A_1 and A_2 anodic peaks, more studies were performed by varying the potential scan rate in acidic solutions of **4-EA**. The results show that the peak current ratio $I_p^{A2}/I_p^{A1}$is related to the potential scan rate and decreases with increasing it. (Fig. 5)

As an important and noteworthy point, it should be mentioned that in the strongly acidic and basic medium, immediately after the salvation of **4-EA**, a percentage of **4-EA** enter the hydrolysis reaction. The hydrolysis reaction is supported by passing different times after the mixing **4-EA** in the strongly acidic and

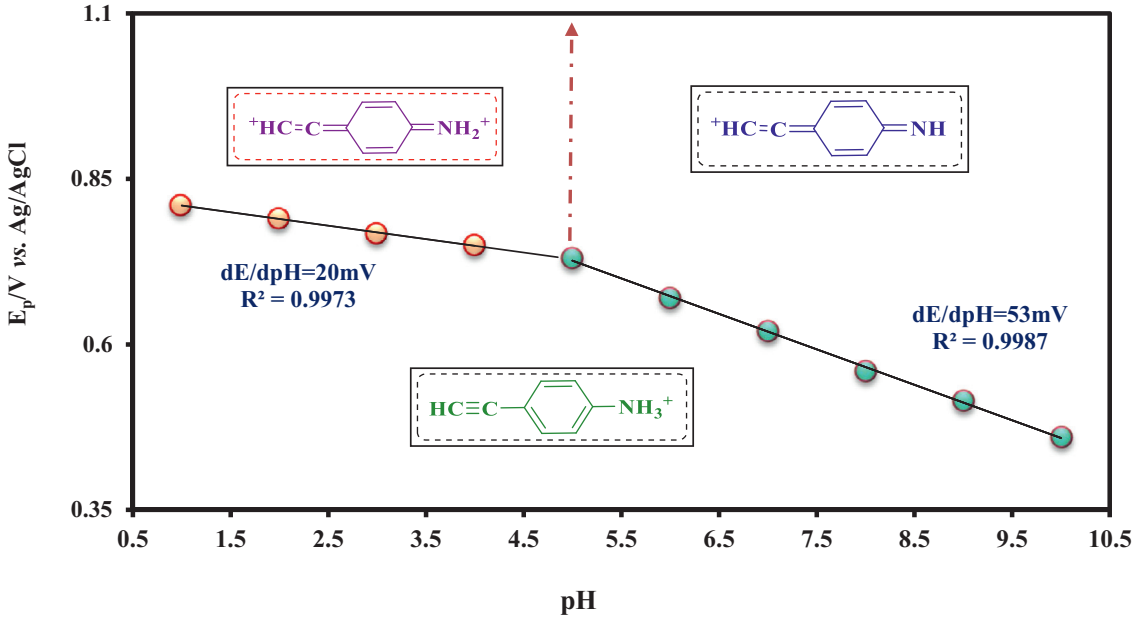

Fig. 3. The potential-pH diagram of **4-EA**.

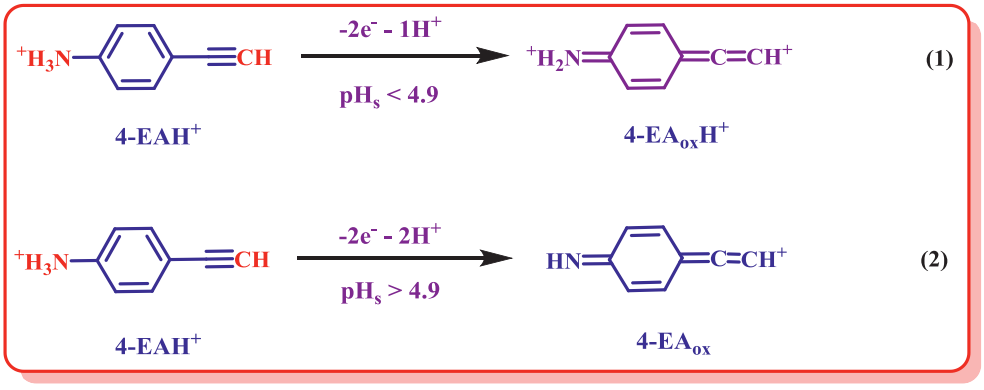

Scheme 1. Oxidation pathways of **4-EA** in different pH values.

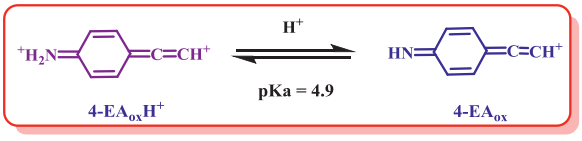

Scheme 2. Acid/base equilibrium of **4-EA$_{ox}$H⁺/4-EA$_{ox}$**.

basic solutions. As shown in Fig 6, in pH: 2.0 with increasing the overtime, anodic peak A_1 decreased and followed by anodic peak A_2 increased continually, indicating that hydrolysis reaction takes place in solution. Anodic peak A_2 is related to the oxidation of **P1** as the product of the hydrolysis reaction. (Scheme 3). Finally, after one hour, the anodic peak A_1 disappears and A_2 reaches its maximum value (Fig. 6). In fact, after one hour, all of the **4-EA** hydrolyzed to the corresponding ketonic form **P1** in a strong acidic and basic medium. Since the ketonic group in **P1** is a more electron-withdrawing group than that acetylenic group [30], the anodic peak of A_2 appeared in more positive potential.

3.3. Controlled-Potential coulometry

Controlled-potential coulometry was implemented in aqueous solution containing 0.1 M HCl, containing **4-EA** (0.25 mmol) at

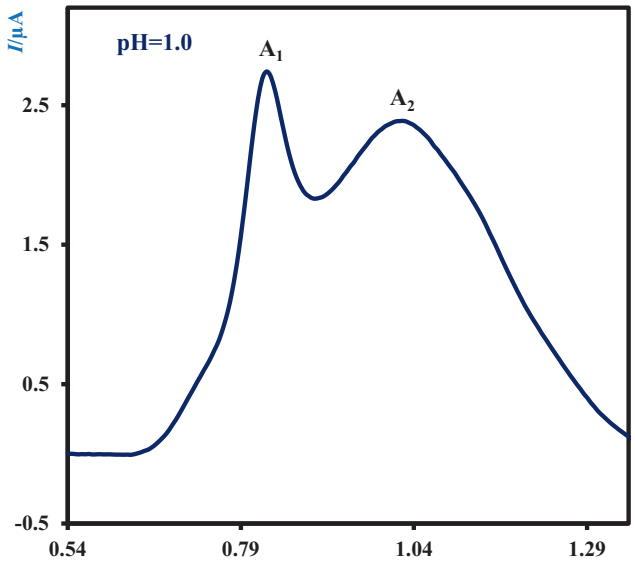

Fig. 4. Differential pulse voltammogram of **4-EA** (1.0 mM) at glassy carbon electrode in a mixture of 0.1 M HCl / acetonitrile (80/20 v/v). Potential scan rate: 10 mV/s. Room temperature.

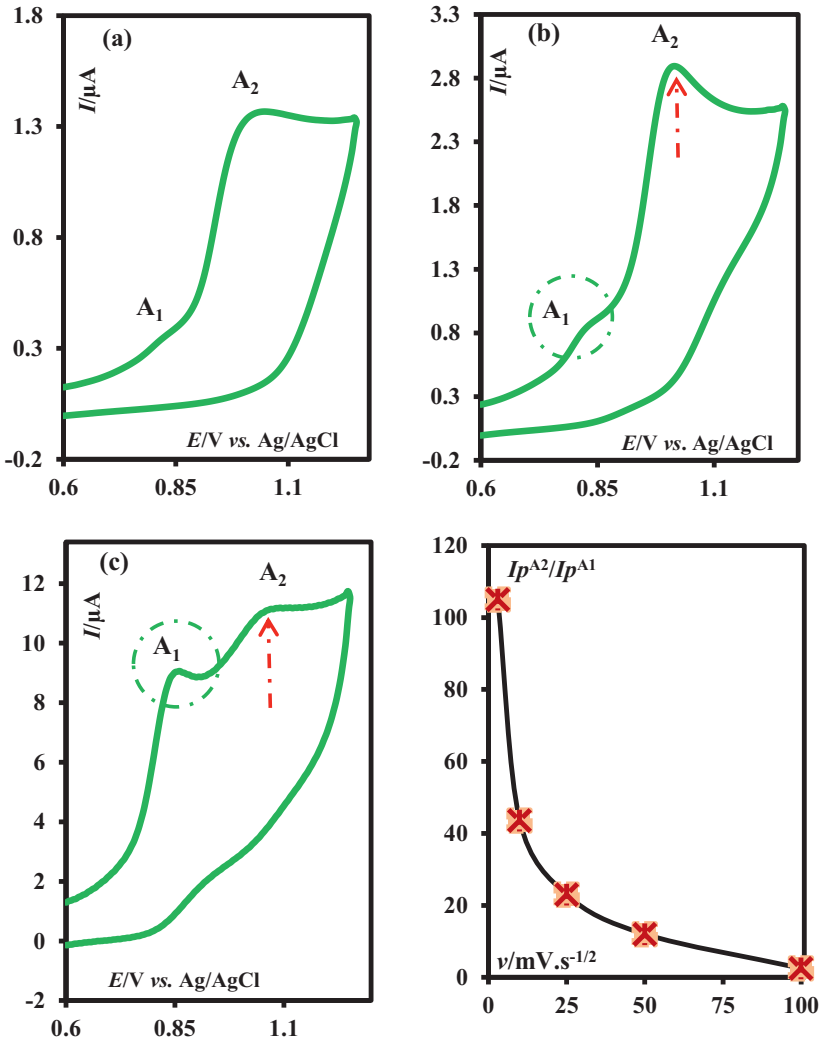

Fig. 5. Cyclic voltammograms of **4-EA** (1.0 mM) at glassy carbon electrode in mixture of buffer solution (pH 2.0, c = 0.2 M) / acetonitrile (80/20 v/v) in different potential scan rates. Potential scan rates from a to c are: 3, 10, and 100 mV/s. (d) variation of peak current ratio for A_1 and A_2 peaks (I_p^{A2}/I_p^{A1}) vs. scan rate. Room temperature.

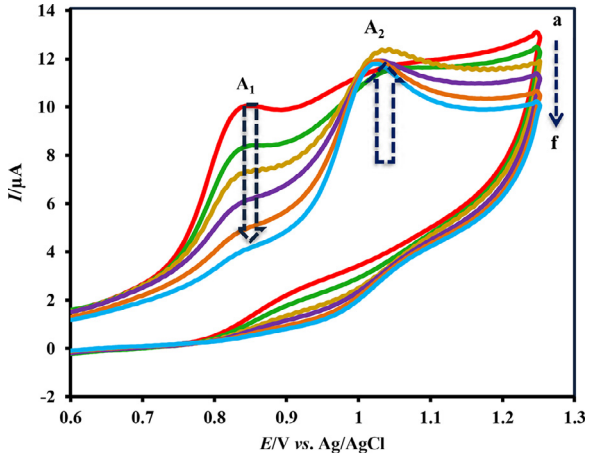

Fig. 6. Cyclic voltammograms of **4-EA** (1.0 mM) at glassy carbon electrode in mixture of buffer solution (pH 2.0, c = 0.2 M) / acetonitrile (80/20 v/v) in different times. Times from a to f are: 0, 10, 20, 30, 40 and 50 s. Potential scan rates: 100 mV/s. Room temperature.

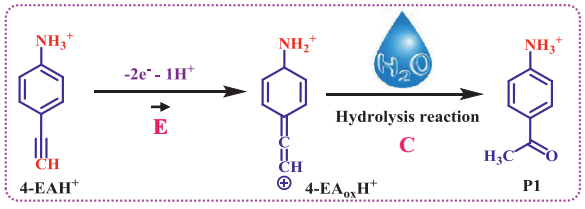

Scheme 3. The proposed mechanism for the formation of **P1** in a strongly acidic pH.

0.87 V versus Ag/AgCl. Using the cyclic voltammetry, the progress of the electrolysis advancement was examined (Fig. 7). It shows that with the growth of the electrolysis, anodic peak A_1 was decreased and finally disappeared at the end of electrolysis. In parallel new anodic peak (A_3) appear in the middle of electrolysis and its current gets rise.

The obtained spectroscopic data (^{13}C NMR, ^{1}H NMR, IR), the molecular mass of 230 for the final product, voltammetry and coulometric studies allow us to propose a mechanism for the electrochemical oxidation of **4-EA** (Scheme 4).

The results revealed that **4-EA was** protonated in the acidic medium and converted to **4-EAH$^+$. 4-EAH$^+$**is oxidized and **4-EA$_{ox}$H$^+$** is formed on the surface of the electrode. The conjugated addition reaction of **4-EA** to **4-EA$_{ox}$H$^+$** leads to **D-4-EA**. Finally, **D-4-EA** oxidized to the final product (**P.2**) *via* a two-electron

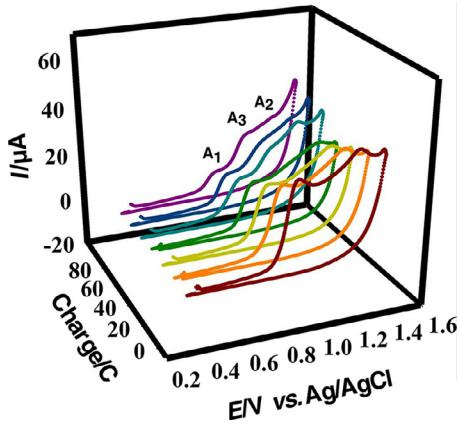

Fig. 7. Cyclic voltammograms of **4-EA** (0.25 mmol) during controlled potential coulometry at 0.87 V versus Ag/AgCl in aqueous solution containing 0.1 M HCl. The consumed charge passed through the cell from a to g are: 0, 15, 30, 45, 60, 75, and 90 coulombs, respectively. Potential scan rates: 100 mV/s. Room temperature.

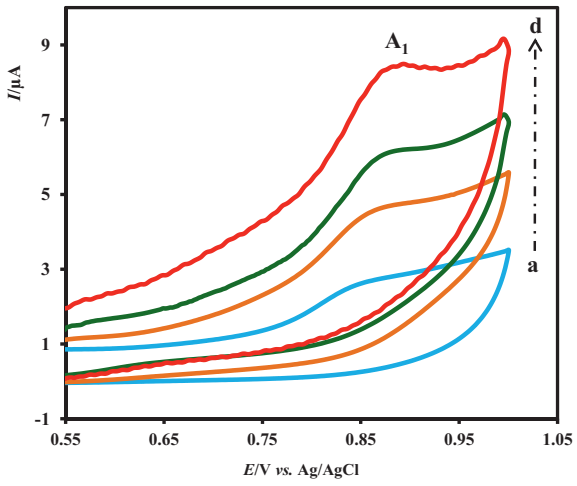

Fig. 8. Cyclic voltammograms of **4-EA** (1.0 mM) at glassy carbon electrode in acetonitrile containing $LiClO_4$ (1.0 M) in different potential scan rates. Potential scan rates from a to d are: 10, 25, 50, and 100 mV/s. Room temperature.

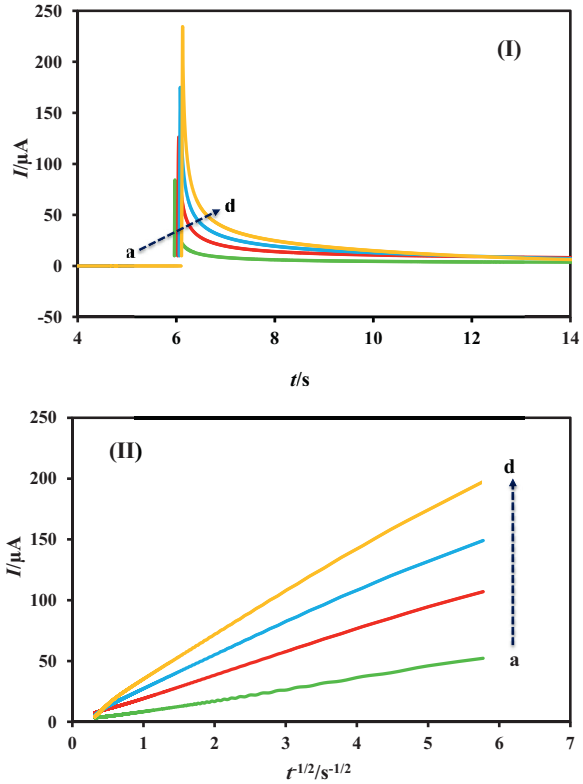

Fig. 10. (**I**) Chronoamperograms of **4-EA** at glassy carbon electrode in acetonitrile containing $LiClO_4$ (1.0 M) in different concentrations of **4-EA**. Concentrations from a to d are: 1.0, 3.0, 5.0 and 7.0 mM. The potential of 0.95 V versus Ag / AgCl was applied for 10 s. (**II**): $I\text{-}t^{-1/2}$ diagrams of **4-EA** for the corresponding point in chronoamperogram **I**. Room temperature.

tow-proton process. The chromatogram of the precipitate obtained from the electrolysis cell shows two spots: Colorless in the above (**P1**) and yellow point in the bottom (**P2**). The separated colorless compound was identified as 1-(4-aminophenyl)ethan-1-one (**P1**), which is similar to the ketonic product obtained from the hydrolysis of **4-EA** as a chemical reaction in strong acidic pHs. The electrochemical synthesis of **P2** was successfully implemented in HCl

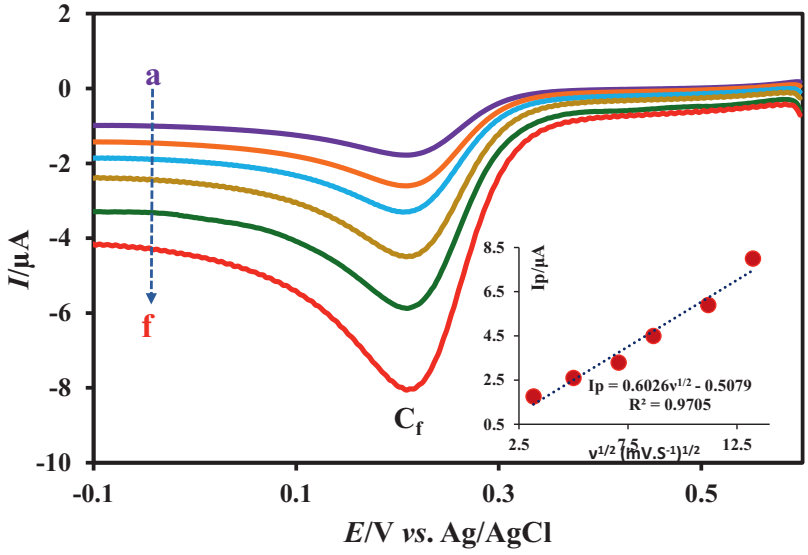

Fig. 9. Linear sweep voltammograms of potassium ferricyanide containing KCl (1.0 M) at glassy carbon electrode in aqueous solution in different potential scan rates. Potential scan rates from a to f are: 10, 25, 50, 75, 125, and 175 mV/s. Room temperature.

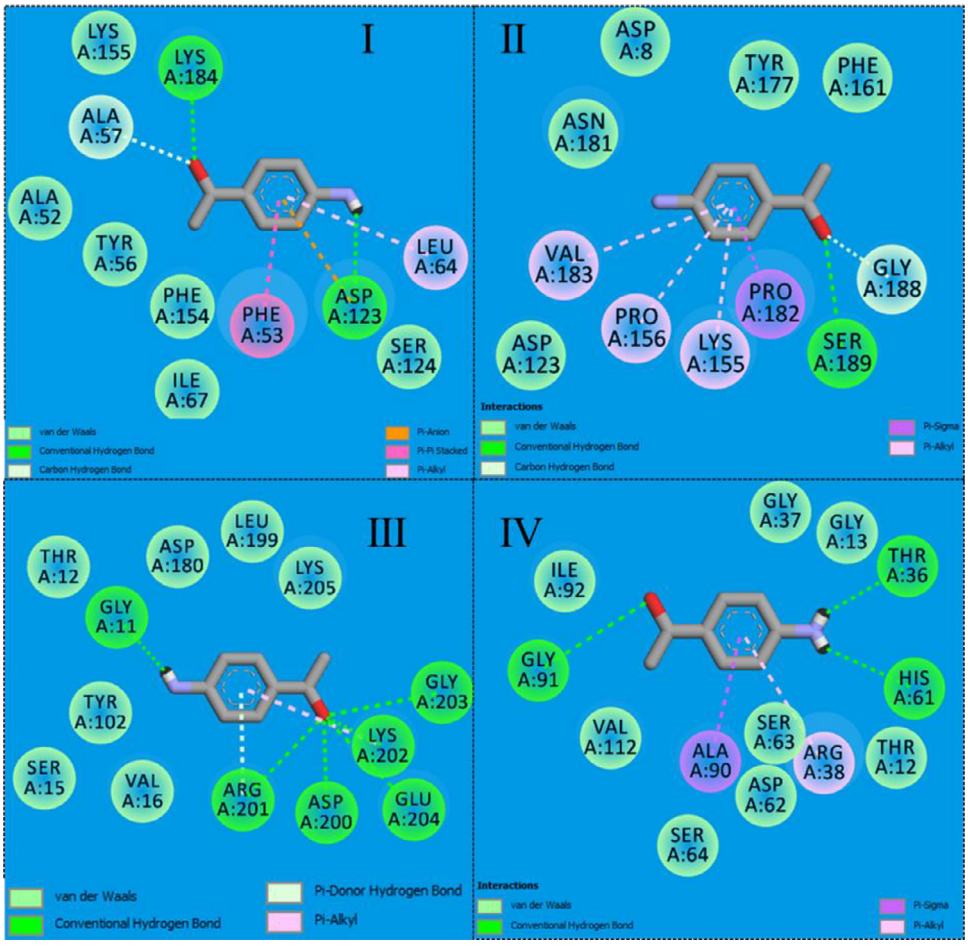

Fig. 11. The binding residues of (**I**) 6Q7N, (**II**) 6Q7R, (**III**) 6Q7P, (**IV**) 1ZK4 with 4-aminoacetophenone.

(0.1 M) in water /ethanol (70/30 v/v) solution (80 ml) at 0.87 V versus Ag/AgCl.

3.4. Chronoamperometry technique and diffusion coefficient of 4-EA

In this section, cyclic voltammograms of **4-EA** (1.0 mM) in acetonitrile containing $LiClO_4$ (1.0 M) in different potential scan rates were recorded. Fig. 8 shows the cyclic voltammograms of **4-EA** (1.0 mM) at different potential scan rates in acetonitrile. Under these conditions, the voltammograms show an irreversible anodic peak (A_1) at 0.85 versus Ag/AgCl in all of the potential scan rates that appurtenant to oxidation of **4-EA**. As can be seen in the comparison of cyclic voltammogram a in Fig. 2, in this situation (in the absence of water), the anodic peak A_2, which corresponds to the hydrolysis reaction of **4-EA$_{ox}$H$^+$**, disappeared.

In continues, the diffusion coefficient of **4-EA** has been measured by the chronoamperometry technique. This method is an important and accurate way to assess diffusion coefficients [31–33]

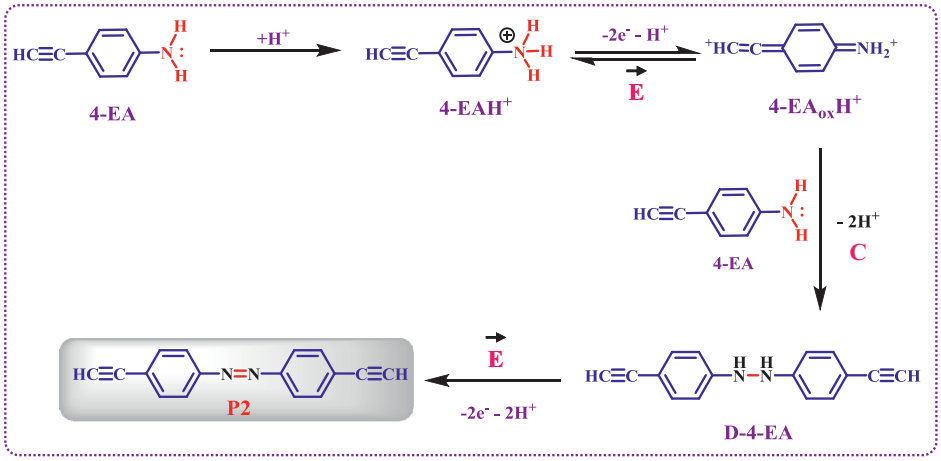

Scheme 4. Proposed mechanism for the electrochemical dimerization pathway of **4-EA**.

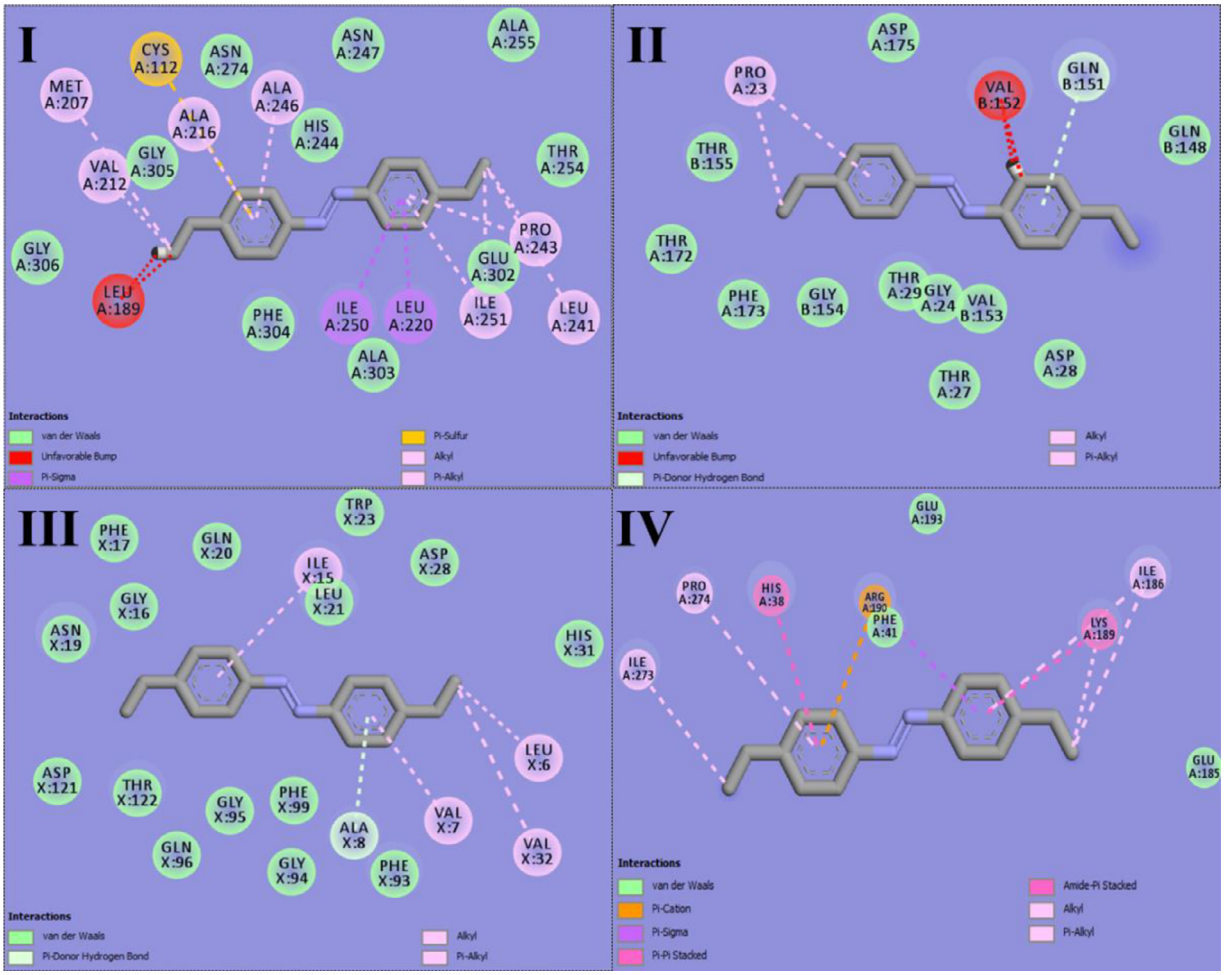

Fig. 12. The binding residues of (**I**) 1HNJ, (**II**) 3FV5, (**III**) 3SRW, (**IV**) 4ZVI with azo compound.

and the rate constants of homogeneous reactions [34,35]. In this path, for using of an equation proposed by Shoup and Szabo [36], at first, the sample was pre-treated by holding the potential at a point corresponding to zero faradic currents for 5 s, after which the potential was stepped to 0.95 V and the current measured for 10 s. Analyzing the time-dependent current response, the current response, i, was obtained over the entire time domain with a maximum error of less than 0.6%.

$$i = -4nFDcr_d f(\tau) \quad (1)$$

$$f(\tau) = 0.7584 + 0.8863\tau^{-1/2} + 0.2146\exp(-0.7823\tau^{-1/2}) \quad (2)$$

The parameter *n, F, c,* and r_d have the meaning described previously [37]. The dimensionless time parameter, τ is given by 37

$$\tau = 4Dt/{r_d}^2$$

Using Shoup and Szabo equation, it should be calculated r_d as the radius of the disk electrode. So, the cathodic scan in linear sweep voltammetry was recorded in a 1.0 mM solution of potassium ferricyanide. In the following, by drawing the $I\text{-}v^{1/2}$ and using the Randles–Sevcik equation (I_p=2.69 × 10^5 × A × $n^{3/2}$ × $D^{1/2}$ × C_0 × $\upsilon^{1/2}$), the radius of the electrode calculated was equal to 0.09 cm (Fig. 9).

In the following, chronoamperograms of **4-EA** in the various concentrations of it and in acetonitrile were recorded. Fig. 10, **I**, shows the chronoamperograms of **4-EA** in different concentrations (1.0, 3.0, 5.0, and 7.0 mM) in acetonitrile.

$I\text{-}t^{1/2}$ diagrams were drawn with choosing a curve with the least adsorption effect (Fig. 9, **II**). The diffusion coefficient of **4-EA** was calculated after analyzing these diagrams and using the equations proposed by Shoup and Szabo's (1.9 × 10^{-6} ± 3.2 × 10^{-7}) [36].

3.5. Molecular modelling

Molecular docking is the most popular approach for investigating interactions between a target (synthesized compounds) and a receptor (enzyme). In this work, molecular modeling of 4-aminoacetophenone (P1) and 1,2-bis(4-ethynylphenyl)hydrazine (P2) and receptors have been performed. Molegro Virtual Docker (MVD), a high accuracy software, was applied for prediction of binding affinity (kj/mol), interactions of aminoacetophenone and 1,2-bis(4-ethynylphenyl)hydrazine binding modes in the receptor binding sites (cavities). For simplification, the highest MolDock Score (kj/mol) was chosen, and other docking results were reported in supporting information. The highest binding affinity (-79.97 kj/mol) was obtained for docking of aminoacetophenone in the BH32 alkylated (PDB ID: 6Q7N) cavities Table 1. The inhibition effect of the synthesized compounds (aminoacetophenone and 1,2-bis(4-ethynylphenyl)hydrazine) is enhanced with a more negative value of binding affinity. Van der Waals, conventional hydrogen bond, carbon-hydrogen bond, Pi-alkyl, and Pi-cation, Pi-anion, Pi-sigma are various interactions formed between functional groups and binding residues. For simplification, the interactions between aminoacetophenone in the BH32 alkylated (PDB ID: 6Q7N) have been reported. Figure 11 conventional hydrogen bonds

Table 1
The binding affinity (kj/mol) of docking results for the 4-aminoacetophenone compound.

Receptors	6Q7N	6Q7R	6Q7P	1ZK4
synthesized compound P1	−79.97	−72.74	−67.78	−61.94

Table 2
The binding affinity (kj/mol) of docking results for the azo compound.

Receptors	1HNJ	3FV5	3SRW	4ZVI
Azo compound	−99.61	−72.91	−102.78	−84.38

were formed between ASP 123, LYS 184 residues, and N, O moieties. The benzene ring has Pi-anion with ASP 123, Pi-Pi stacked with PHE 53, and Pi-alkyl with LEU 64. The results indicated that 4-aminoacetophenone (P1) has a positive effect on receptors like acetophenone. For the azo compound (P2), the high antibacterial activity is related to molecular docking of 3SRW with the binding affinity -102.15 kj/mol (Table 2). Some interactions such as Van der Waals, alkyl, Pi-alkyl, Pi-cation, Pi-sulfur, Pi-sigma, Pi-donor hydrogen bond, Pi-Pi stacked, and amid-Pi stacked are detected via docking of the azo compound with relevant receptors (Fig. 12). For 3SRW, two alkyls and two Pi-alkyl interactions are formed between LEU 6, VAL 32, and ILE 15, VAL 7, respectively. The result indicated that all receptors have an inhibitory effect on the activity of desired Bactria.

4. Conclusions

For the first time, the electrochemical oxidation of 4-ethynylaniline (**4-EA**) was investigated in different pH values. Our data show that **4-EA** has different behavior depends on pH values. In these situations, **4-EA** can participate in oxidation and hydroxylation reactions depend on the solution's pH. Also, the potential-pH diagram of **4-EA** was constructed and used to investigate the property of various kinds of **4-EA** and calculation of oxidation form pK_a in a mixture of buffer solution/acetonitrile. In the next step, a new derivative of azo compounds was also synthesized. This electrosynthesis procedure was performed at room temperature in the single step, facile conditions, using simple undivided cell and the use of electrons instead of oxidizing reagents. For biological assessment, the molecular docking of some receptors and 1,2-bis(4-ethynylphenyl) diazene have been performed. The results show that azo product has an inhibitory effect against receptors. Finally, the diffusion coefficient of **4-EA** was calculated in pure acetonitrile.

Declaration of Competing Interest

None.

Acknowledgment

We are pleased to acknowledge the support of this investigation by Bu-Ali Sina University Research Council and Iran's National Elites Foundation.

Supplementary materials

Supplementary material associated with this article can be found, in the online version, at doi:10.1016/j.electacta.2021.138242.

Referecnes

[1] F. Diederich, P.J. Stang, R.R. Tykwinski, Acetylene Chemistry: Chemistry, Biology and Material Science, Wiley-VCH, Weinheim, 2006.
[2] J.H.P. Utley, R. Lines, The Electrochemistry of the Carbon-Carbon Triple Bond, John Wiley & Sons, 1978 byPart 2, Volume 2, doi:10.1002/9780470771570.
[3] J. Zhou, X. Zh. Tao, J.J. Dai, C.G. Li, J. Xu, H.M. Xu, H.J. Xu, Electrochemical synthesis of 1,2-diketones from alkynes under transition-metal-catalyst-free conditions, Chem. Commun. 55 (2019) 9208–9211.
[4] L. Gobbi, N. Elmaci, H.P. Lüthi, F. Diederich, N-Dialkylaniline-Substituted N, Tetraethynylethenes: a new class of chromophores possessing an emitting charge-transfer state. experimental and computational studies, Phys. Chem. Chem. Phys. 2 (2001) 423–433.
[5] M. Schreiber, R.R. Tykwinski, F. Diederich, R. Spreiter, U. Gubler, C. Bosshard, I. Poberaj, P. Günter, C. Boudon, J.P. Gisselbrecht, M. Gross, Tetraethynylethene molecular scaffolding: nonlinear optical, redox, and amphiphilic properties of donor functionalized polytriacetylene and expanded radialenes, Adv. Mater. 9 (1997) 339–343.
[6] P. Reutenauer, M. Kivala, P.D. Jarowski, C. Boudon, J.P. Gisselbrecht, M. Gross, F. Diederich, New strong organic acceptors by cycloaddition of TCNE and TCNQ to donor-substituted cyanoalkynes, Chem. Commun. 46 (2007) 4898–4900.
[7] Y. Huang, X. Chong, C. Liu, Y. Liang, B. Zhang, Boosting hydrogen production via anodic oxidation of primary amines over a NiSe nanorod electrode, Angew. Chem. Int. Ed. 57 (2018) 13163–13166.
[8] H. Liu, C. Xu, D. Li, H.L. Jiang, Photocatalytic hydrogen production coupled with selective benzylamine oxidation over MOF composites, Angew. Chem. Int. Ed. 57 (2018) 5379–5383.
[9] F. Su, S.C. Mathew, L. Mohlmann, M. Antonietti, X. Wang, S. Blechert, Aerobic oxidative coupling of amines by carbon nitride photocatalysis with visible light, Angew. Chem. Int. Ed. 50 (2011) 657–660.
[10] N.M. Aljamali, Zetasizer technique in biochemistry, Biochem. Anal. Biochem. 4 (2015) 1–5.
[11] Y. Zang, I. Stone, M.S. Inkpen, F. Ng, T.H. Lambert, C. Nuckolls, M.L. Steigerwald, X. Roy, L. Venkataraman, *In situ* coupling of single molecules driven by Au-catalyzed electrooxidation, Angew. Chem. Int. Ed. 58 (2019) 16008–16012.
[12] X. Chong, C. Liu, Y. Huang, Ch. Huang, B. Zhang, Potential-tuned selective electrosynthesis of azoxy-, azo- and amino-aromatics over a CoP nanosheet cathode, Natl. Sci. Rev. 7 (2020) 285–295.
[13] Y. Liang, W. Zhou, Y. Shi, C. Liu, B. Zhang, Unveiling *in situ* evolved In/In_2O_{3-x} heterostructure as the active phase of In_2O_3 toward efficient electroreduction of CO_2 to formate, Sci. Bull. 65 (2020) 1547–1554.
[14] N.M. Rageh, Electronic Spectra, Solvatochromic behavior and acid-base properties of some azo cinnoline compounds, Spectrochim. Acta Part A Mol. Biomol. Spectrosc. 60 (2004) 103–109.
[15] K.V. Bernaerts, F.E. Du Prez, Dual/heterofunctional initiators for the combination of mechanistically distinct polymerization techniques, Prog. Polym. Sci. 31 (2006) 671–722.
[16] H.F. Mark, N.M. Bikales, C.G. Overberger, G. Menges (Eds.), Encyclopedia of Polymer Science and Engineering, Vol. 2, Wiley, New York, 1985.
[17] J.T. Spadaro, Biological and chemical degradation of azo dyes under aerobic conditions, in: M. (Howe-Grant (Ed.), Kirk-Othmer Encyclopedia of Chemical Technology, 4th ed., John Wiley and Sons, New. York, 1992, pp. 678–679. Vol. 8.
[18] S.A. Ibrahim, A.M. Hammam, A.M. Kamal El-Dean, A.A. Mohamed, N.M. Rageh, Tautomeric structures, electronic spectra, and acid-base properties of some hydroxy-azopyrazolopyridines, Can. J. Appl. Spectrosc. 38 (1993) 1–6.
[19] G.P. Warwick, Relative rates of reduction of a series of azo compounds, J. Soc. Dye. Colour. 75 (1959) 291–299.
[20] W.C.J. Ross, G.P. Warwick, Reduction of cytotoxic azo compounds by hydrazine and by the xanthine oxidase–xanthine system, Nature 176 (1955) 298–299.
[21] M. Patel, A.Amin T.Shah, Therapeutic opportunities in colon-specific drug-delivery systems, Crit. Rev. Ther. Drug Carrier Syst. 24 (2007) 147–202.
[22] A. Jain, Y. Gupta, S.K. Jain, Perspectives of biodegradable natural polysaccharides for site-specific drug delivery to the colon, J. Pharm. Pharm. Sci. 10 (2007) 86–128.
[23] U. Klotz, M. Schwab, Topical delivery of therapeutic agents in the treatment of inflammatory Bowel disease, Adv. Drug Deliv. Rev. 57 (2005) 267–279.
[24] G. Mooter, B. Maris, C. Samyn, P. Augustijns, R.J. Kinget, Use of azo polymers for colon-specific drug delivery, J. Pharmacol. Sci. 86 (1997) 1321–1327.
[25] D.A. Kennedy, N. Vembu, F.R. Fronczek, M. Devocelle, Synthesis of mutual azo prodrugs of anti-inflammatory agents and peptides facilitated by α-aminoisobutyric acid, J. Org. Chem. 76 (2011) 9641–9647.
[26] M. Jamshidi, S. Torabi, M. Tavan, A. Azizi, S. Khazalpour, Electrochemical behavior and LC-MS analysis of anthocyanin's in vaccinium arctostaphylos L. extract: the molecular modelling of potential inhibition to COVID-19 and ROS generation receptors, J. Electrochem. Soc. 167 (2020) 155505.
[27] P. Amooshahi, S. Khazalpour, A. Amani, Electrochemical evidence in mechanism of toxicity of mefenamic acid overdose in the presence of glutathione and N-acetyl-L-cysteine, J. Electrochem. Soc. 167 (2020) 045503.
[28] P.Amooshahi K.Wahedi, M. Jamshidi, S. Khazalpour, Electrochemical assessment of EC and ECE mechanisms for caffeic acid in the presence of aromatic amines, Anal. Bioanal. Chem. Res. 7 (2020) 345–353.
[29] A. Molegro, MVD 5.0 Molegro Virtual Docker. DK-8000, Aarhus C, Denmark, 2011.
[30] T. Curtius, Ueber die einwirkung von salpetriger Säure auf salzsauren glycocoläther, Ber. Dtsch. Chem. Ges. 16 (1883) 2230–2231.
[31] W. Hyk, A. Nowicka, Z. Stojek, Direct determination of diffusion coefficients of substrate and product by chronoamperometric techniques at microelectrodes for any level of ionic support, J. Anal. Chem. 74 (2002) 149–157.

[32] J.V. Macpherson, P.R. Unwin, Determination of the diffusion coefficient of hydrogen in aqueous solution using single and double potential step chronoamperometry at a disk ultramicroelectrode, J. Anal. Chem. 69 (1997) 2063–2069.
[33] H. Ikeuchi, M. Kanakubo, Chronoamperometry at small disk electrodes, J. Electroanal. Chem. 493 (2000) 93–99.
[34] M.L. Olmstead, R.S. Nicholson, Double potential step method for measuring rate constants of dimerization reactions, Anal. Chem. 41 (1969) 851–852.
[35] A. Bewick, D. Serve, T.A. Joslin, Anodic oxidation of aromatic nitrogen compounds. Spectroelectrochemical studies of EE AND EEC, processes with a coupled redox reaction, J. Electroanal. Chem. 154 (1983) 81–105.
[36] D. Shoup, A. Szabo, Chronoamperometric current at finite disk electrodes, J. Electroanal. Chem. Interfacial Electrochem. 140 (1982) 237–245.
[37] R. Wibowo, L. Aldous, E.I. Rogers, S.E. Ward Jones, R.G. Compton, A study of the Na/Na^+ redox couple in some room temperature ionic liquids, J. Phys. Chem. C 114 (2010) 3618–3626.